Int. J. Solids Structures Vol. 21, No. 11, pp. 1117–1129, 1985
Printed in Great Britain.

0020–7683/85 $3.00 + .00

A CLASS OF PLASTIC CONSTITUTIVE EQUATIONS WITH VERTEX EFFECT—II. DISCUSSIONS ON THE SIMPLEST FORM

MANABU GOTOH
Department of Precision Engineering, Gigu University, Yanagido 1-1, Gifu-City, 501-11, Japan

(*Received* 1 *August* 1983)

Abstract—The simplest form of the plastic constitutive equations developed in Part I is presented together with its inverse expression with respect to rigid–plastic and elastic–plastic materials. Discussions on the behavior of the material with this constitutive equation are made. Delay-phenomenon and its rather quick recovery of the direction of stress after a corner of strain-path, and drop in the stress–strain curve at the corner are confirmed to appear. It is found that severe nonproportionality in strain-path makes stresses in the material get comparatively lower than that for J_2-flow theory. In simple shear, shearing stress reaches its maximum value almost immediately after the onset of local-type bifurcation, and then decreases monotonically and slowly with shearing.

1. INTRODUCTION

In Part I[1], general theory on a new type of plastic constitutive equations was developed. Here some detailed discussions on the simplest form of them are presented. Namely, discussion is presented on the rigid–plastic form and its inverse expression, the elastic–plastic form and its inverse expression, the half angle of the pointed vertex cone of the subsequent loading surface and on the behavior of the material just after a sudden change of stress- or strain-path. An application to simple shearing is also given.

2. RIGID–PLASTIC CONSTITUTIVE EQUATIONS

Here we concern ourselves with the following plastic constitutive equation which is described in Part I[1] as the simplest form of those developed there:

$$\mathrm{d}\mathbf{e}^p = [\langle P(\Theta)\rangle/2h_0][a\,\mathring{\mathrm{d}}\mathbf{T} + b(\mathbf{T}/\bar{\sigma})\,\overline{\mathrm{d}\sigma}], \tag{1}$$

where

$\mathrm{d}\mathbf{e}^p = \mathrm{d}\boldsymbol{\epsilon}^p - (1/3)(\mathrm{tr}\,\mathrm{d}\boldsymbol{\epsilon}^p)\mathbf{I}$,
$\mathrm{d}\boldsymbol{\epsilon}^p$ = increment of plastic strain,
$\mathbf{I}$ = unit tensor of second rank,
$\mathbf{T} = \boldsymbol{\sigma} - (1/3)(\mathrm{tr}\,\boldsymbol{\sigma})\mathbf{I}$,
$\boldsymbol{\sigma}$ = Cauchy stress,
$\mathring{\mathrm{d}}\mathbf{T}$ = Jaumann increment of $\mathbf{T} = \mathrm{d}\mathbf{T} - \mathrm{d}\boldsymbol{\omega}\mathbf{T} + \mathbf{T}\,\mathrm{d}\boldsymbol{\omega}$,
$\bar{\sigma} = \sqrt{3/2}(\mathrm{tr}\,\mathbf{T}^2)^{1/2}$,
$\overline{\mathrm{d}\sigma} = \sqrt{3/2}(\mathrm{tr}\,\mathring{\mathrm{d}}\mathbf{T}^2)^{1/2}$,
h_0, H_0 = instantaneous work-hardening and vertex-hardening rates for proportional loadings, respectively,
$\mathrm{d}\boldsymbol{\omega}$ = increment of rigid-body rotation,
Θ = angle between $\mathbf{T}$ and $\mathring{\mathrm{d}}\mathbf{T}$ in the five-dimensional deviatoric stress space[1],

$$\cos\Theta = \mathrm{tr}(\mathbf{T}\,\mathring{\mathrm{d}}\mathbf{T})/[(\mathrm{tr}\,\mathbf{T}^2)(\mathrm{tr}\,\mathring{\mathrm{d}}\mathbf{T}^2)]^{1/2}, \tag{2}$$

$$P(\Theta) = a + b\cos\Theta, \tag{3}$$

$\langle P\rangle = P$ for $P > 0$,
$= 0$ for $P \leqq 0$,
$a = h_0/H_0$; $b = 1 - a$,

and $h_0 = (1/3)\,\overline{\mathrm{d}\sigma}/\overline{\mathrm{d}\epsilon^p}$ for a proportional loading, i.e. the slope of stress–strain curve divided by 3, where

$$\overline{\mathrm{d}\epsilon}^p = \sqrt{2/3}(\mathrm{tr}\,\mathrm{d}\boldsymbol{\epsilon}^{p2})^{1/2}.$$

If the stress-path is controlled, the expression (1) can be directly used. On the other hand, if the strain-path is controlled, its inverse expression is needed, which will soon be derived below.

From eqn (1) and eqns (24), (33) and (34) in Part I, we can easily find that

$$a = h_0/H_0 = \cos\Theta_0/(1 + \cos\Theta_0), \tag{4}$$

$$\Theta_0 = \pi - \Theta_{\max}$$

$$= \text{half angle of the vertex-cone of subsequent loading surface,} \tag{5}$$

$$\Theta_{\max} = \cos^{-1}(-a/b), \tag{6}$$

and therefore if

$$0 \leqq \Theta < \Theta_{\max} \tag{7}$$

holds, then plastic deformation will continue for subsequent stress increment $\mathring{\mathrm{d}}\mathbf{T}$.

Making scalar products of both sides of eqn (1) and dividing them by $(\overline{\mathrm{d}\epsilon}^p)^2$, we obtain the following relations:

$$h = (1/3)\,\overline{\mathrm{d}\sigma}/\overline{\mathrm{d}\epsilon}^p = \bar{h}_0/P(\Theta), \tag{8}$$

$$\bar{h}_0 = h_0/(a^2 + 2ab\cos\Theta + b^2)^{1/2}, \tag{9}$$

where plastic loading is assumed to continue, i.e. $P(\Theta) > 0$. Of course, for $\Theta = 0$ (proportional loadings, say), $h_0 = \bar{h}_0 = h$ hold.

Defining the angle θ^p between $\mathbf{T}$ and $\mathrm{d}\boldsymbol{e}^p$ by the equation

$$\cos\theta^p = \mathrm{tr}(\mathbf{T}\,\mathrm{d}\boldsymbol{e}^p)/[(\mathrm{tr}\,\mathbf{T}^2)(\mathrm{tr}\,\mathrm{d}\boldsymbol{e}^{p2})]^{1/2}$$

$$= \mathrm{tr}(\mathbf{T}\,\mathrm{d}\boldsymbol{e}^p)/(\bar{\sigma}\,\overline{\mathrm{d}\epsilon}^p), \tag{10}$$

we obtain the following expression for $\cos\theta^p$:

$$\cos\theta^p = (b + a\cos\Theta)/(a^2 + 2ab\cos\Theta + b^2)^{1/2}, \tag{11}$$

which relates θ^p to Θ. This relation is valid for any form of the function $P(\Theta)$.

From eqns (4)–(7) and (11), we find that

$$0 \leqq \theta^p < \theta^p_{\max} < \pi/2, \tag{12}$$

$$\theta^p_{\max} = \Theta_{\max} - (\pi/2),$$

$$\sin\theta^p_{\max} = \cos\Theta_{\max} = -a/b. \tag{13}$$

From eqn (13), it is confirmed that the range of the direction of $\mathrm{d}\boldsymbol{e}^p$ is confined within the cone which makes a right angle to the loading surface cone as illustrated in Fig. 1, which is very reasonable. If $H_0 = \infty$, or for $\Theta = 0$, from eqn (11), θ^p is equal to 0, which is also reasonable. The inverse expression of eqn (11) is written as

$$\cos\Theta = (1/a)(-b\sin^2\theta^p + \cos\theta^p\sqrt{a^2 - b^2\sin^2\theta^p})$$

$$= [-\sin^2\theta^p + \cos\theta^p(\sin^2\theta^p_{\max} - \sin^2\theta^p)^{1/2}]/\sin\theta^p_{\max}. \tag{14}$$

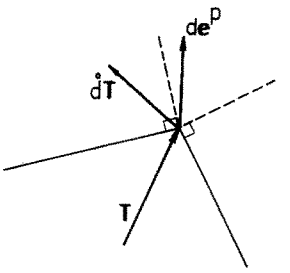

Fig. 1. Vertexed loading surface and range of direction of plastic strain increment.

This equation gives an indefinite cos Θ for $H_0 \to \infty$ ($b \to 1$, $a \to 0$) except for $\theta^p = 0$. That is, the direction of $\mathbf{de}^p$ is restricted to the direction of $\mathbf{T}$ for the case of smooth loading surface. The relation between Θ and θ^p is also given by the following expression:

$$\Theta = \theta^p + \psi^p; \qquad \psi^p = \sin^{-1}\{(b/a)\sin\theta^p\}. \tag{15}$$

The function $P(\Theta)$ and $\bar{h}_0$ in eqn (9) are expressed in terms of θ^p as follows:

$$\begin{aligned} P(\Theta) &= (1/a)\sqrt{a^2 - b^2\sin^2\theta^p}(b\cos\theta^p + \sqrt{a^2 - b^2\sin^2\theta^p}) \\ &= b\sqrt{\sin^2\theta^p_{\max} - \sin^2\theta^p}(\cos\theta^p + \sqrt{\sin^2\theta^p_{\max} - \sin^2\theta^p})/\sin\theta^p_{\max}, \end{aligned} \tag{16}$$

$$\bar{h}_0 = h_0/[b(\cos\theta^p + \sqrt{\sin^2\theta^p_{\max} - \sin^2\theta^p})]. \tag{17}$$

Making use of eqns (16) and (17), we can obtain the following inverse expression of the constitutive equation (1):

$$\begin{aligned} \mathring{\mathbf{d}}\mathbf{T} &= 2H_0[\mathbf{de}^p - (3\bar{h}_0/2h_0)b(\mathbf{T}/\bar{\sigma})\,\overline{\mathbf{de}}^p]/P(\Theta) \\ &= 2h_0[\mathbf{de}^p - (3/2)(\mathbf{T}/\bar{\sigma})\,\overline{\mathbf{de}}^p/(\cos\theta^p + \sqrt{\sin^2\theta^p_{\max} - \sin^2\theta^p})]/ \\ &\quad [b^2\sqrt{\sin^2\theta^p_{\max} - \sin^2\theta^p}(\cos\theta^p + \sqrt{\sin^2\theta^p_{\max} - \sin^2\theta^p})]. \end{aligned} \tag{18}$$

This equation implies that, if $\theta^p = 0$, then $\mathring{\mathbf{d}}\mathbf{T} = 2h_0\,\mathbf{de}^p$. And if $H_0 \to \infty$, or for a nonhardening material whose h_0 is equal to 0, θ^p and $\theta^p_{\max}$ must be equal to 0 for continuing plastic deformation and $\mathring{\mathbf{d}}\mathbf{T}$ gets indefinite. For $\mathbf{de}^p$ of $\theta^p = \theta^p_{\max}$, if $\overline{\mathbf{de}}^p$ has nonzero value, $\mathring{\mathbf{d}}\mathbf{T}$ cannot but be indefinite, which implies that no plastic deformation is possible for such direction of $\mathbf{de}^p$. These are all reasonable.

3. ELASTOPLASTIC CONSTITUTIVE EQUATION

Combining isotropic elasticity with eqn (1), we have the following elastoplastic constitutive equation:

$$\mathbf{de} = \mathbf{de}^e + \mathbf{de}^p = (1/2G^*)\,\mathring{\mathbf{d}}\mathbf{T} + [b\langle P(\Theta)\rangle/2h_0](\mathbf{T}/\bar{\sigma})\,\overline{\mathbf{d}\sigma}, \tag{19}$$

where

$\mathbf{de}^e$ = increment of elastic deviatoric strain,
$\mathbf{de}$ = increment of total deviatoric strain = $\mathbf{d}\epsilon - (1/3)(\mathrm{tr}\,\mathbf{d}\epsilon)\mathbf{I}$,
$\mathbf{d}\epsilon$ = increment of total strain,

$$1/G^* = 1/G + \langle P(\Theta)\rangle/H_0, \tag{20}$$

and G is the elastic rigidity modulus. If we put as

$$\overline{\mathbf{d}\epsilon} = \sqrt{2/3}(\mathrm{tr}\,\mathbf{d}\epsilon^2)^{1/2}; \qquad \overline{\mathbf{de}}^e = \sqrt{2/3}(\mathrm{tr}\,\mathbf{de}^{e2})^{1/2}, \tag{21}$$

then, for a proportional loading, we have the following relation:

$$\overline{d\epsilon} = \overline{d\epsilon}^e + \overline{d\epsilon}^p, \qquad \text{(proportional loading)}. \tag{22}$$

Therefore we can find that

$$1/h_0 = (1/\bar{h}_0) - (1/G), \tag{23}$$

where we put $3\bar{h}_0 = \overline{d\sigma}/\overline{d\epsilon}$ for a proportional loading. $\bar{h}_0$ is evaluated from the experimental $\bar{\sigma}$–$\bar{\epsilon}$ curve, where

$$\bar{\epsilon} = \int \overline{d\epsilon}.$$

Then h_0 is easily estimated from eqn (23).

On the other hand, for an arbitrary loading, we put $3\bar{h} = \overline{d\sigma}/\overline{d\epsilon}$. Then, making scalar products of both sides of eqn (19) divided by $\overline{d\epsilon}^2$, we obtain the following expression:

$$h_0/\bar{h} = [(\gamma + a\langle P\rangle)^2 + 2(\gamma + a\langle P\rangle)b\langle P\rangle \cos\Theta + (b\langle P\rangle)^2]^{1/2}, \tag{24}$$

where $\gamma = h_0/G$. From this equation, we can confirm easily that

$\bar{h} = G$ for elasticity,
$= h$ for rigid plasticity,
$= \bar{h}_0$ for $\Theta = 0$,
$= 1/[(1/G)^2 + (2/hG)\cos\Theta + (1/h)^2]^{1/2}$ for $H_0 \to \infty$.

Now let us define the angle θ between $\mathbf{T}$ and $\mathbf{de}$ by the equation

$$\cos\theta = \mathrm{tr}(\mathbf{T}\,\mathbf{de})/(\bar{\sigma}\,\overline{d\epsilon}), \tag{25}$$

then, from eqn (19), we find that

$$\cos\theta = \{(\gamma + a\langle P\rangle)\cos\Theta + b\langle P\rangle\}/[(\gamma + a\langle P\rangle)^2 + 2\langle P\rangle(\gamma + a\langle P\rangle)b\cos\Theta + (b\langle P\rangle)^2]^{1/2}. \tag{26}$$

From this equation, it is easily seen that $\theta = 0$ for $\Theta = 0$. And, for $\Theta = \Theta_{\max}$, i.e. $\cos\Theta = -a/b$, then $P = 0$ and thus $\cos\theta = \cos\Theta_{\max} = -a/b$. Therefore, we reach the following interesting result:

$$\theta_{\max} = \Theta_{\max} = \cos^{-1}(-a/b). \tag{27}$$

That is, for a subsequent strain increment $\mathbf{de}$, if

$$0 \leqq \theta < \theta_{\max} = \Theta_{\max} \tag{28}$$

holds, then plastic deformation continues. This result is completely different from the condition described in eqn (12) for rigid–plastic case, which is, of course, due to elastic part of strain increment.

The inverse expression of the elastoplastic constitutive equation (19) is readily written as follows:

$$\mathring{d}\mathbf{T} = 2G^*[\mathbf{de} - (3/2)\langle P\rangle(\bar{h}/h_0)b(\mathbf{T}/\bar{\sigma})\,\overline{d\epsilon}]. \tag{29}$$

However, the right-hand side of this expression involves cos Θ. For strain-path control case, de is given at any stage of deformation and thus cos θ is known due to eqn (25). Then cos Θ must be evaluated by solving eqn (26). In practice, this can be easily done by a direct numerical method varying the value of cos Θ from $(-a/b)$ to 1, stepwise, to find out its exact value. When no value of cos Θ within the range $[-a/b, 1]$ is found, then the state changes from plastic to elastic range, i.e. unloading takes place. [Or, in numerical analysis of deformation by incremental method, if nonproportionality of the strain-path is not very severe, we may use the value of cos Θ evaluated in just one step earlier calculation, taking appropriately small increments, though all the numerical examples described below are obtained by use of the direct solution of eqn (26).]

From eqn (26), we find that

$$\begin{aligned} \Theta &= \theta + \psi, \qquad (0 \leqq \psi \leqq \pi/2) \\ \sin\psi &= (b/a)\sin\theta\cdot\{1 - [\gamma/(a\langle P\rangle + \gamma)]\}. \end{aligned} \tag{30}$$

We denote Θ by $\Theta_\perp$ for a special case of $\theta = \pi/2$. Then

$$\theta = \pi/2, \qquad \psi = \Theta_\perp - (\pi/2). \tag{31}$$

Therefore from eqn (30) we find that, for plastic state,

$$(b/a)\{1 - \gamma/[a(a + b\cos\Theta_\perp) + \gamma]\} = -\cos\Theta_\perp, \tag{32}$$

$$\begin{aligned} \cos\Theta_\perp &= -(1/2)\alpha(1 - \sqrt{1 - (2/\alpha)^2}); \qquad \pi/2 \leqq \Theta_\perp, \\ \alpha &= (b/a) + (a/b) + (\gamma/ab) \geqq 0. \end{aligned} \tag{33}$$

In eqn (32), $1 - (2/\alpha)^2 > 0$ always holds. When no vertex forms on the loading surface, then $a \to 0$, $(b/a) \to \infty$, $(a/b) \to 0$, $(\gamma/ab) \to \infty$ and $\alpha \to \infty$. Then according to Apostol's theorem, $\cos\Theta_\perp \to -0$ and thus $\Theta_\perp \to +\pi/2$. For $\gamma \to 0$, from eqn (32), $\cos\Theta_\perp \to (-a/b)$. Therefore, for $\gamma \ll 1$, from eqn (32), we find that

$$\langle P\rangle \fallingdotseq \gamma a/(b^2 - a^2), \qquad (\gamma \ll 1, \theta = \pi/2). \tag{34}$$

Therefore from eqn (30),

$$\Theta_\perp \fallingdotseq (\pi/2) + \sin^{-1}(a/b), \qquad (\gamma \ll 1). \tag{35}$$

Conversely, we denote θ by $\theta_\perp$ for a special case of $\Theta = \pi/2$. For this case, from eqn (26), we find that

$$\cos\theta_\perp = ab/[(\gamma + a^2)^2 + a^2b^2]^{1/2} > 0 \tag{36}$$

and thus $0 < \theta_\perp \leqq \pi/2$, in which the equality is for the case of no-vertex ($a \to 0$, $b \to 1$). If $\gamma \ll 1$, from eqn (36), we have

$$\cos\theta_\perp \fallingdotseq b/\sqrt{a^2 + b^2}, \qquad (\gamma \ll 1). \tag{37}$$

Finally, in addition to eqn (19) or (29), we have the following constitutive equation for the volumetric part:

$$\mathrm{tr}\, d\boldsymbol{\epsilon} = (1/3K)\,\mathrm{tr}\, d\boldsymbol{\sigma}, \tag{38}$$

where incompressible plasticity is assumed and K denotes the elastic bulk modulus.

4. DISCUSSION ON Θ_0

The material coefficients which have to be determined by the basic experiments in the constitutive equations (1), (18) or (19), or (29) and (38), are h_0, H_0, Θ_0 and/or G and K. There is no difficulty in measurement of the elastic moduli G and K. h_0 is also easily evaluated from uniaxial tensile test (say) as mentioned earlier. Furthermore, h_0/H_0 is expressed in terms of Θ_0 as in eqn (4). Therefore if Θ_0 is formulated, then the constitutive equations are completely constructed.

Generally speaking, the loading (or the initial yield) surface may be considered to be smooth for a loading of arbitrary direction before yielding. In fact, even in Tresca material, there exist initial pointed vertices or corners only at a few special directions of loading. Therefore it is most reasonable and general for us to understand in a manner such that a vertex, if it will, forms and develops with plastic deformation after yielding takes place as illustrated schematically in Fig. 2. Representing the magnitude of plastic deformation by the length of the plastic strain-path ϵ, namely

$$\epsilon = \int \overline{d\epsilon^p}, \tag{39}$$

and assuming that Θ_0 is even in ϵ, Θ_0 is formulated most simply as $\Theta_0 = \pi/2 - \rho\epsilon^2$, where ρ is a new material constant which governs the rate of vertex development. This formula is, however, evidently unreasonable when ϵ gets large so that Θ_0 gets too small or even negative. Consequently, we formulate it as follows:

$$\begin{aligned} \Theta_0 &= (\pi/2) - \rho\epsilon^2, \quad \text{for} \quad 0 \leqq \epsilon < \epsilon^*, \\ &= \Theta^* \quad \text{(const)}, \quad \text{for} \quad \epsilon^* \leqq \epsilon, \end{aligned} \tag{40}$$

where, of course, $\Theta^* = (\pi/2) - \rho\epsilon^{*2}$. Θ^* denotes the stationary vertex angle after some degree of plastic deformation. This idea that the vertex angle will get to be stationary with plastic deformation is now very common to the workers who believe such vertex formation on the loading surface to occur (see, e.g. [2]). Equation (40) is illustrated schematically in Fig. 3(a).

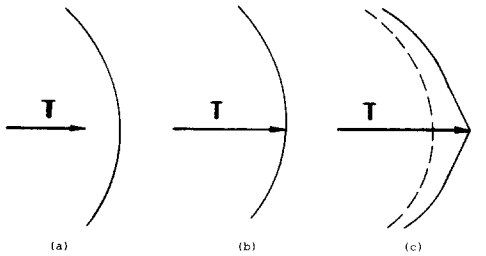

Fig. 2. Evolution of pointed vertex at the loading point on the loading surface: (a) before yielding; (b) onset of yielding; (c) plastic loading.

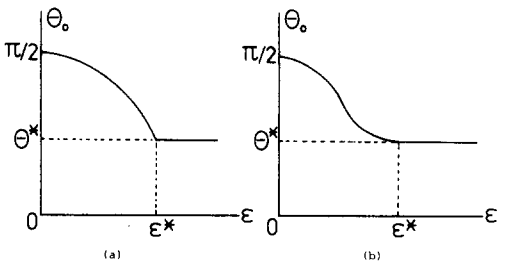

Fig. 3. Variation of half angle Θ_0 of vertexed loading surface cone with ϵ: (a) eqn (40); (b) eqn (41).

More precisely, eqn (40) can be revised into the following form:

$$\begin{aligned} \Theta_0 &= (\pi/2) - \rho\epsilon^2 + (\rho/2\epsilon^{*2})\epsilon^4, \quad \text{for} \quad 0 \leqq \epsilon < \epsilon^*, \\ &= \Theta^*, \quad \text{for} \quad \epsilon^* \leqq \epsilon \end{aligned} \tag{41}$$

where $\Theta^* = (\pi/2) - (\rho\epsilon^{*2}/2)$. This formula is illustrated in Fig. 3(b).

The author has confirmed by several applications that the value of ϵ^* can be set 0.7–0.8, and thus the single formula $\Theta_0 = (\pi/2) - \rho\epsilon^2$ is valid in most deformation problems. The formulae (40) and (41) will be referred for more severe deformation problems.

5. A FEW DISCUSSIONS IN PLANE-STRESS STATE

Let us consider a plane-stress state where tensile stress σ_{11} and shearing stress τ_{12} act. Denoting T_{11} by s, and T_{12} by τ, we have $T_{22} = T_{33} = -s/2$ and other $T_{ij} = 0$. Furthermore, putting $\tau^* = (2/\sqrt{3})\tau$, we know that the circle expressed by the following equation represents the Mises' yield locus on $(s\text{–}\tau^*)$ plane:

$$s^2 + \tau^{*2} = k^2 \ (= \text{const}). \tag{42}$$

And we have

$$\begin{aligned} (2/3)\bar{\sigma} &= \sqrt{2/3}(\text{tr}\,\mathbf{T}^2)^{1/2} = (s^2 + \tau^{*2})^{1/2}, \\ \mathring{\bar{\sigma}}/\bar{\sigma} &= (9/4)(s\mathring{s} + \tau^*\mathring{\tau}^*)/\bar{\sigma}^2. \end{aligned} \tag{43}$$

On the other hand, putting $e_{11} = e$, and $(2/\sqrt{3})e_{12} = \gamma^*$, from eqn (19) we obtain the following equations:

$$\begin{aligned} \dot{e} &= (1/2G^*)\mathring{s} + (b\langle P\rangle/2h_0\bar{\sigma})s, \\ \dot{\gamma}^* &= (1/2G^*)\mathring{\tau}^* + (b\langle P\rangle/2h_0\bar{\sigma})\tau^*. \end{aligned} \tag{44}$$

If we use the rate type of J_2-deformation theory in its hypoelastic version due to Stören and Rice[3], the relations corresponding to those in eqn (44) are expressed as follows:

$$\begin{aligned} \dot{e} &= \{(1/2G) + \delta\cdot[Cs^2 + (1/2H_0)]\}\mathring{s} + \delta\cdot Cs\tau^*\mathring{\tau}^*, \\ \dot{\gamma}^* &= \delta\cdot Cs^*\mathring{s} + \{(1/2G) + \delta\cdot[C\tau^{*2} + (1/2H_0)]\}\mathring{\tau}^*, \\ C &= /2h_0\bar{\sigma}^2, \end{aligned} \tag{45}$$

where $\delta = 1$ for plastic loading; $\delta = 0$ for unloading or elastic state.

If we use J_2-flow theory, the relations reduced by $H_0 \to \infty$ in eqn (44) or (45) are obtained.

Now let us consider the behavior of the material just after a sudden change of stress-path. For example, for a change from unaxial tension of $s \neq 0$ and $\tau = 0$ ($\dot{e} \neq 0$ and $\dot{\gamma}^* = 0$) to pure shear of $\mathring{s} = 0$ and $\mathring{\tau}^* \neq 0$, we know that Θ is equal to $\pi/2$ and thus eqn (44) reduces to

$$\begin{aligned} \dot{e} &= ab(1/2h_0\bar{\sigma})s, \\ \dot{\gamma}^* &= [(1/2G) + (a/2H_0)]\mathring{\tau}^*, \end{aligned} \tag{46}$$

and eqn (45) reduces to

$$\begin{aligned} \dot{e} &= 0, \\ \dot{\gamma}^* &= [(1/2G) + (1/2H_0)]\mathring{\tau}^*. \end{aligned} \tag{47}$$

Therefore, the response of the material with the constitutive equation (19) is evidently different from that of the material obeying J_2-deformation theory or J_2-flow theory. Of course, if $H_0 \to \infty$, no difference in the responses appears and unloading takes place.

In this case, $s\mathring{s} + \tau^*\mathring{\tau}^* = 0$ and thus $d\bar{\sigma} = 0$ holds. Therefore, for both of the constitutive equation (19) and J_2-deformation theory, $(\bar{\sigma} - \bar{\epsilon})$ curve will get parallel to the $\bar{\epsilon}$-axis at the stress-path change, whereas for J_2-flow theory unloading takes place.

Next, when strain-path is abruptly changed from $\dot{e} \neq 0$ and $\dot{\gamma}^* = 0$ ($s \neq 0$ and $\tau^* = 0$) to $\dot{e} = 0$ and $\dot{\gamma}^* \neq 0$, i.e. $\theta = \pi/2$, eqn (44) gives the following equations at the instant of the path change:

$$\begin{aligned} \mathring{s} &= -2G^*\langle P\rangle(b/2h_0\bar{\sigma})s, \\ \mathring{\tau}^* &= 2G^*\dot{\gamma}^*. \end{aligned} \tag{48}$$

From this equation we obtain the following expression:

$$\begin{aligned} d\bar{\sigma}/\overline{d\sigma} &= -2G^*\langle P\rangle(b/2h_0\bar{\sigma}^2)s^2 < 0, \\ P &= a + b\cos\Theta_\perp, \qquad [\Theta_\perp\text{: due to eqn (33)}]. \end{aligned} \tag{49}$$

This implies that the $(\bar{\sigma}$–$\bar{\epsilon})$ curve drops at the point of the strain-path change of $\theta = \pi/2$.

On the other hand, corresponding to eqn (48), eqn (45) gives the following equations:

$$\begin{aligned} \mathring{s} &= 0, \\ \mathring{\tau}^* &= \dot{\gamma}^*\{(1/2G) + (C/2H_0)\}, \end{aligned} \tag{50}$$

which gives $d\bar{\sigma}/\overline{d\sigma} = 0$. Namely, for J_2-deformation theory, the $(\bar{\sigma}$–$\bar{\epsilon})$ curve gets parallel to $\bar{\epsilon}$-axis at the strain-path change of $\theta = \pi/2$. J_2-flow theory predicts again that unloading (more exactly, neutral loading) takes place at this instant.

The experimental results for similar conditions by several workers tell us that such abrupt change of strain-path induces a pronounced drop in the $(\bar{\sigma}$–$\bar{\epsilon})$ curve as predicted by use of the constitutive equation proposed here (see, e.g. [4–5]).

6. NUMERICAL EXAMINATIONS OF THE MATERIAL BEHAVIOR

Several typical responses of the material whose constitutive equation is expressed by eqn (19) or (29) are numerically examined for three types of strain-path. The material constants are taken as follows:

$$\begin{aligned} G &= 82.5\text{ GPa}, \qquad \nu\text{ (Poisson's ratio)} = 0.29 \\ \sigma_0 &= 24.7\text{ MPa} \end{aligned} \tag{51}$$

where σ_0 is the initial yield stress beyond which n-th power law is used as the expression of work-hardening characteristics, i.e.

$$\bar{\sigma} = F\cdot\bar{\epsilon}^n, \qquad \text{(proportional loadings)} \tag{52}$$

in which

$$\begin{aligned} n &= 0.333 = \text{work-hardening exponent or } n\text{-value}, \\ F &= 592\text{ MPa}, \end{aligned}$$

and the new material constant ρ is chosen as

$$\rho = 0.922.$$

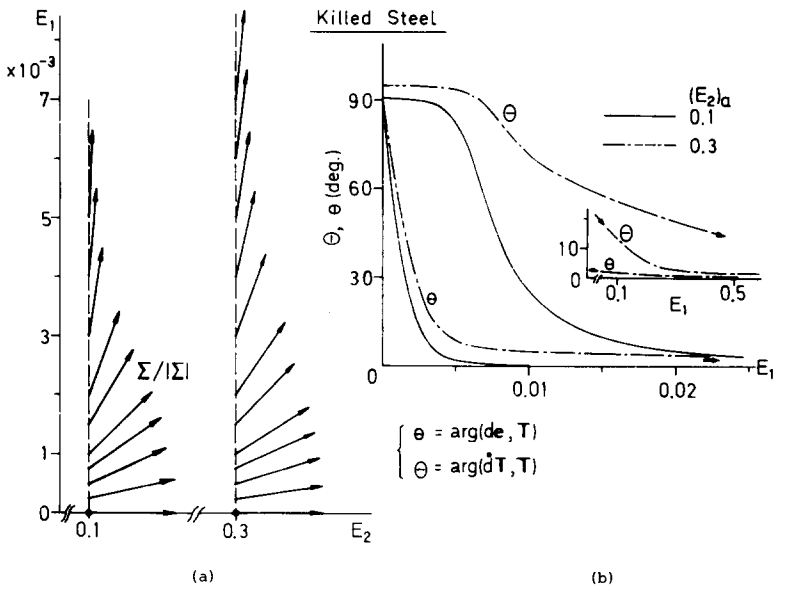

Fig. 4. Theoretical material behavior after corner of strain-path: (a) variation of stress direction; (b) variation of θ and Θ.

These values are all those for a kind of aluminium-killed steel sheet and determined by the experiments. Particularly, the value of ρ is determined so that the theoretical breakage strain of the steel sheet subjected to equibiaxial tension due to localized necking coincides with the experimental value. (Extensive investigations on the breakage strain of various kinds of metal sheet will appear in Part III.)

First, we examine how the direction of stress will vary with deformation after an abrupt change of strain-path. Introducing the following denotations[6],

$$E_1 = e_{11}$$
$$E_2 = (e_{11} + 2e_{22})/\sqrt{3}; \qquad \mathbf{E} = (E_1, E_2) \tag{53}$$

$$\Sigma_1 = (3/2)T_{11}$$
$$\Sigma_2 = (\sqrt{3}/2)(T_{11} + 2T_{22}); \qquad \mathbf{\Sigma} = (\Sigma_1, \Sigma_2) \tag{54}$$

The material is first strained uniformly along the strain-path of $E_1 = 0$, up to $E_2 \fallingdotseq 0.1$ and 0.3. Then, without unloading, the strain-path is abruptly changed to $dE_1 \neq 0$ and $dE_2 = 0$, and then kept to deform along the second straight strain-path. The results are illustrated in Fig. 4(a), where the arrows with the constant normalized length which emanate from the corresponding points in the strain-space show the direction of stress. From this figure, it is clear that the coaxiality between $\mathbf{\Sigma}$ and $d\mathbf{E}$, or $\mathbf{T}$ and $\mathbf{de}$, does not hold at the strain-path change, but rather quickly it is recovered with deformation. This phenomenon is nowadays well known by the experiments[4–7] and called "the delay-phenomenon" of the stress direction. Denoting E_2 by $(E_2)_a$ at the path change, we find that the recovery of such coaxiality takes place quicker for smaller value of $(E_2)_a$. (We should note that J_2-flow theory requires always the coaxiality between $\mathbf{T}$ and $\mathbf{de}^p$ which is almost equivalent to that between $\mathbf{T}$ and $\mathbf{de}$.)

Figure 4(b) illustrates how the angles θ and Θ vary with deformation after the strain-path change. Note that θ is equal to $\pi/2$ at the instant of the path change, whereas Θ is more than $\pi/2$ without unloading. This aspect of variation of θ is also very similar to that verified by the experiments (see, e.g. [6]).

Figure 5 illustrates the stress–strain curves corresponding to Fig. 4. In this figure, the solid curves show the ($\bar{\sigma}$ vs $\bar{\epsilon}$) relation for proportional loading and the chain curves are those for (σ_A–$\bar{\epsilon}$) after the strain-path change, where $\bar{\sigma}$ is calculated simply from

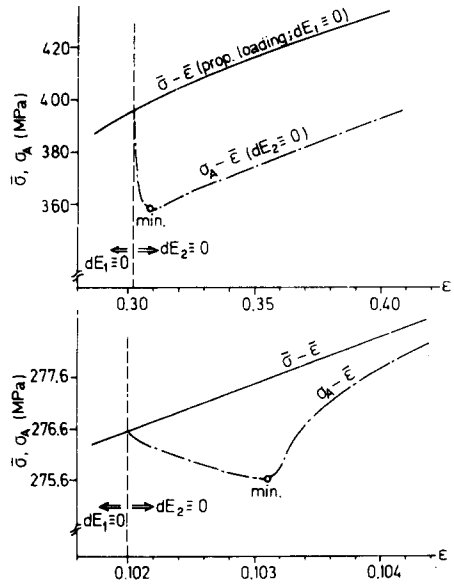

Fig. 5. Stress–strain curves corresponding to Fig. 4.

eqn (52) using only $\bar{\varepsilon}$ which is given in this case, and σ_A is the actual $\bar{\sigma} = \sqrt{3/2}(\mathrm{tr}\,\mathbf{T}^2)^{1/2}$ whose $\mathbf{T}$ is evaluated by the equation

$$\mathbf{T}_i = \mathbf{T}_{i-1} + d\mathbf{T}_i, \tag{55}$$

where i denotes the number of the incremental calculation step, and $d\mathbf{T}_i$ is evaluated from the constitutive equation (29).

In Fig. 5, the drop of σ_A just after the strain-path change is clearly seen. Such phenomenon was also predicted qualitatively in the previous section. Similar experimental evidences are also found in several literatures (see, e.g. [4–7]).

Figure 6(a) illustrates the variation of the direction of stress along the circular strain-paths. Again the arrows show the directions of stress. We should note that J_2-flow theory requires the arrows to be tangential everywhere to the circles. Therefore, in this figure, the delay-phenomenon is again clearly seen. Similar results by the experiments are also found in the literature such as [7]. The author also has attained

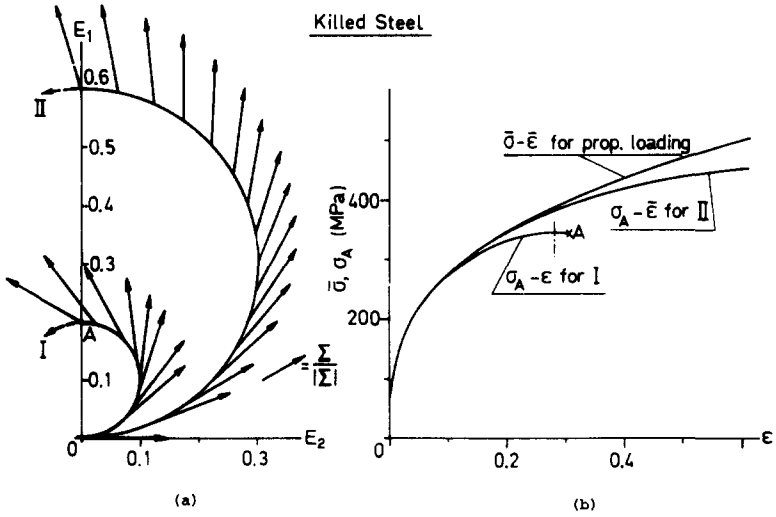

Fig. 6. Theoretical material behavior along circular strain-path: (a) variation of stress direction; (b) stress–strain curves corresponding to (a).

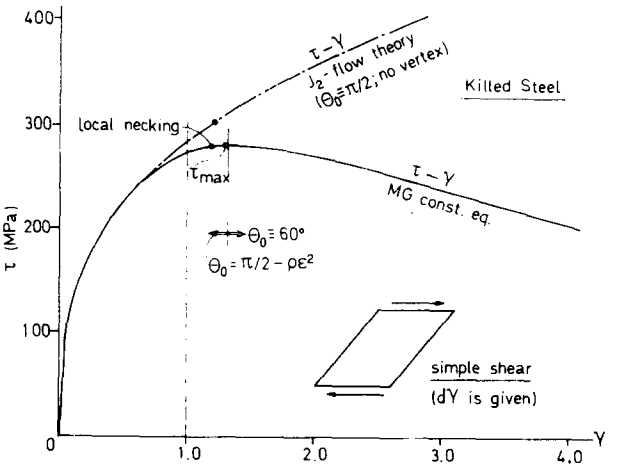

Fig. 7. (τ–γ) curves for simple shear.

similar data by a finite element analysis using a polycrystalline plate model composed of 121 crystal grains[8].

Figure 6(b) illustrates σ_A–$\bar{\epsilon}$ curves corresponding to Fig. 6(a). We see that the stress level for circular strain-paths is comparatively lower than that for proportional loading. [Note that J_2-flow theory follows of course ($\bar{\sigma}$–$\bar{\epsilon}$) curve.] Therefore, the effect of vertex-formation should be understood to play a significant role, not only in bifurcation problems as reported by several workers[3, 9–11], but also in stress analyses; especially in the case where severe nonproportionality of loading predominates.

Finally, we examine the material behavior under simple shear. A plane-strain block or a thin sheet is subjected to simple shearing strain γ whose increment $d\gamma$ ($= 2d\epsilon_{12}$) is given for every step of numerical calculation. Then, according to the constitutive equation (29), stress increments are evaluated. Here eqn (40) is used for the expression of Θ_0 in which Θ^* is assumed to be 60°. Figure 7 illustrates (τ–γ) curve so obtained, in which for comparison that for a proportional loading or for any loading of materials obeying J_2-flow theory is also drawn. The curve for our material reaches its maximum point at γ between 1 and 2 and then monotonically and slowly decreases, though the curve for J_2-flow theory continues of course to increase. As Lee pointed out[12], the material with kinematic hardening will give the (τ–γ) curve which oscillates with a

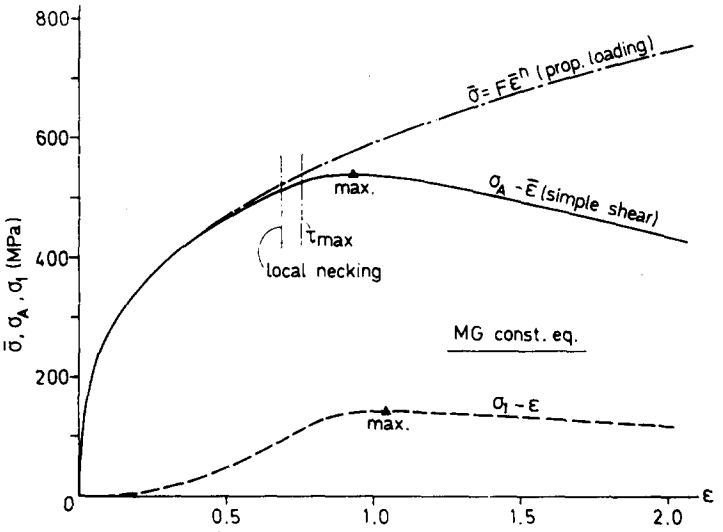

Fig. 8. Stress–strain curves corresponding to Fig. 7.

wavelength of $\Delta\gamma \fallingdotseq 2$. To avoid this difficulty, he revised the form of the so-called rest stress which characterizes the Prager's kinematic-hardening model.

Although it looks rather peculiar that (τ–γ) curve of our material descends with deformation, we should note that it may happen in a very large strain range in which some change of internal structure, such as void formation, would deteriorate the validity of a single form of the constitutive equation (29). Moreover, we can find that the so-called localized type of bifurcation[9–11] takes place just before the maximum point of τ. We have checked this point by the similar method as that used by Stören and Rice[3] or Needleman[13], and plotted it in the figure. After this bifurcation point, localized plastic flow can occur, and stable and uniform simple shearing will cease to continue. However, we neglected this effect in our calculation here. Therefore such descending (τ–γ) curve as that obtained here is very probable. Consequently, so far there seems to exist no need of any modificaton of our constitutive equation.

Figure 8 illustrates (σ_A–$\bar{\epsilon}$) and (σ_1–$\bar{\epsilon}$) curves of our material corresponding to Fig. 7, where σ_1 stands for σ_{11}. (Note $\sigma_{22} = -\sigma_{11}$.) A similar aspect is seen in (σ_A–$\bar{\epsilon}$) curve as that in (τ–γ) curve. The value of σ_{11} is not negligible, though that for J_2-flow theory is very small and not shown in the figure.

7. CONCLUSION

Discussions on the simplest form of the constitutive equations developed in Part I are presented. Rigid–plastic constitutive equation and its inverse expression, and elastoplastic constitutive equation and its inverse expression are completely formulated. For that, the half angle Θ_0 of the vertexed cone of subsequent loading surface is formulated as a simple even function of ϵ (= length of plastic strain-path). Behaviors of the elastoplastic material with this constitutive equation are examined with respect to the strain-path with a corner, the circular strain-path and a severe simple shear. Delay-phenomenon in the direction of stress and its quick recovery after the corner, drop in the stress–strain curve at the corner, both of which are nowadays well known by the experiments, are clearly observed. Such delay-phenomenon is confirmed to occur also for circular strain-paths. On a circular strain-path, the material shows a comparatively lower stress level than that for J_2-flow theory, which implies that the effect of vertex formation appears not only in bifurcation problems, but also in stress analyses, especially for the case where nonproportionality of loading predominates. In simple shearing, the value of shear stress τ reaches its maximum almost immediately after the localized bifurcation, and then decreases monotonically and slowly with shear strain γ, which is very different from the behavior of the material obeying J_2-flow theory which gives monotonically increasing τ, or kinematic-hardening law which gives oscillatory τ.

REFERENCES

1. M. Gotoh, A class of plastic constitutive equation with vertex effect—I. General theory. *Int. J. Solids Structures* **21**, 1101 (1985).
2. J. Christoffersen and J. W. Hutchinson, A class of phenomenological corner theories of plasticity. *J. Mech. Phys. Solids* **27**, 465 (1979).
3. S. Stören and J. R. Rice, Localized necking in thin sheets, *J. Mech. Phys. Solids* **23**, 421 (1975).
4. Y. Ohashi, M. Tokuda and H. Yamashita, Effect of third invariant of stress behavior on plastic deformation of mild steel. *J. Mech. Phys. Solids* **23**, 295 (1975).
5. E. Shiratori, K. Ikegami and K. Kaneko, Stress and plastic strain increment after corners on strain paths, *J. Mech. Phys. Solids* **23**, 325 (1975).
6. Y. Ohashi, Effects of complicated deformation history on inelastic deformation behavior of metals. *Mem. Fac. Eng. Nagoya Univ.* **34**, 1–76 (1982).
7. V. S. Lensky, Analysis of plastic behavior of metals under complex loading. *Plasticity*, p. 259. Pergamon, New York (1960).
8. M. Gotoh, A computer simulation of metal plasticity with the aid of a polycrystalline plate model. *Proc. 22nd Jpn Cong Mater Res.* p. 1 (1979).
9. V. Tvergaard, A. Needleman and K. K. Lo, Flow localization in the plane strain tensile test. *J. Mech. Phys. Solids* **29**, 115 (1981).

10. N. Triantafyllidis, A. Needleman and V. Tvergaard, On the development of shear bands in pure bending. *Int. J. Solids Structures* **18,** 121 (1982).
11. M. Larsson, A. Needleman, V. Tvergaard and B. Storåkers, Instability and failure of internally pressurized ductile metal cylinders. *J. Mech. Phys. Solids* **30,** 121 (1982).
12. E. H. Lee, Finite deformation effects in plasticity analysis. *Numerical Methods in Industrial Forming Processes*, p. 39. Pineridge Press, location (1982).
13. A. Needleman, Non-normality and bifurcation in plane strain tension and compression. *J. Mech. Phys. Solids* **27,** 231 (1979).